



## Original

# A novel, simplified, and reproducible porcine model of acute ischemic liver failure with portal vein preservation

Weisong XUE<sup>1)</sup>, Yu FU<sup>1)</sup>, Haojie ZHANG<sup>1)</sup>, Guoping LI<sup>3)</sup>, Peihua CAO<sup>4)</sup>, Yang LI<sup>1)</sup>, Qing PENG<sup>1)</sup>, Kebo ZHONG<sup>1)</sup>, Shuangtang FENG<sup>3)</sup> and Yi GAO<sup>1,2)</sup>

<sup>1)</sup>General Surgery Center, Department of Hepatobiliary Surgery II, Guangdong Provincial Research Center for Artificial Organ and Tissue Engineering, Guangzhou Clinical Research and Transformation Center for Artificial Liver, Institute of Regenerative Medicine, Zhujiang Hospital, Southern Medical University, No. 253, Gongye Road, Haizhu District, Guangzhou 510280, Guangdong Province, P.R. China

<sup>2)</sup>State Key Laboratory of Organ Failure Research, Southern Medical University, No. 1023, Shatai Road, Baiyun District, Guangzhou 510050, Guangdong Province, P.R. China

<sup>3)</sup>Beijing Grand Lifescience & technology, Ltd., No. 8, Shengmingyuan Road, Changping District, Beijing 100000, P.R. China

<sup>4)</sup>Clinical Research Center, Zhujiang Hospital, Southern Medical University, No. 253, Gongye Road, Haizhu District, Guangzhou 510280, Guangdong Province, P.R. China

**Abstract:** The current ischemic models of liver failure are difficult and usually time-consuming to produce. The aim of this study was to develop a simplified and reproducible porcine model of acute liver failure for use in preclinical research. Eighteen Bama miniature pigs were randomly divided into Groups A, B, and C. The hepatic artery and common bile duct were ligated in all groups. While the portal vein was completely preserved in Group A, it was narrowed by 1/3 and 1/2 in Groups B and C, respectively. Results of biochemical analyses, encephalopathy scores, and survival times were compared among the groups. Results of hematoxylin-eosin staining, terminal deoxynucleotidyl transferase-mediated dUTP nick-end labeling, Masson staining, and Ki-67 analyses were recorded. Survival times in Groups B and C were  $11.67 \pm 1.86$  and  $2.16 \pm 0.75$  days, respectively, shorter than that in Group A (>15 days). Following surgery, alanine aminotransferase, aspartate aminotransferase, lactate dehydrogenase, alkaline phosphatase, total bilirubin, and direct bilirubin levels significantly increased relative to baseline values in all groups ( $P < 0.05$ ). Groups B and C exhibited a significant decrease in encephalopathy scores and a significant increase in ammonia levels, which were negatively correlated with one another. Pathological analysis revealed obvious necrosis of liver cells, which correlated closely with the degree of portal vein constriction. Our simple, highly reproducible model effectively mimics the clinical characteristics of acute liver failure in humans and provides a foundation for further research on artificial liver support system development.

**Key words:** large animal model, liver failure, liver ischemia, pig

## Introduction

Liver transplantation is an important procedure for the treatment of end-stage liver disease [1], but many patients die while waiting for a suitable donor due to the ever-widening gap between supply and demand for do-

nor livers [2]. Recently, researchers focused on a novel alternative to liver transplantation by shifting their attention to artificial liver support systems (ALSS) [3], with a focus on bioartificial liver support systems that can perform biological functions such as synthesis and metabolism [3–6]. Therefore, stable animal models of

(Received 25 April 2021 / Accepted 13 August 2021 / Published online in J-STAGE 8 September 2021)

Corresponding authors: K. Zhong. email: zhongkb@smu.edu.cn

S. Feng. email: fst@grand-lifescience.com

Y. Gao. email: drgaoy@126.com

Supplementary Figure: refer to J-STAGE: <https://www.jstage.jst.go.jp/browse/expanim>



This is an open-access article distributed under the terms of the Creative Commons Attribution Non-Commercial No Derivatives (by-nc-nd) License <<http://creativecommons.org/licenses/by-nc-nd/4.0/>>.

human liver failure need to be established to evaluate the safety, technical applicability, and therapeutic effects of these emerging therapeutic technologies.

Currently, animal models of liver failure are mainly grouped into the following two categories: hepatotoxic drugs and surgical models. Pharmaceutical models have been widely used due to their simplicity and convenience [7, 8] but they have limitations [9], including poor reproducibility, induction of organ damage outside the liver, and potential risks and hazards for experimental personnel. In addition, the effects of hepatotoxic drugs on bioartificial livers remain unknown [10, 11]. Surgical models are developed by hepatectomy or hepatic devascularization (i.e., ischemia models). Total hepatectomy (i.e., the anhepatic model) can rapidly lead to liver failure [12] but cannot mimic the inflammation and release of toxic substances that occur during clinical hepatocyte necrosis and therefore is rarely performed. In addition, the procedure is difficult, and the therapeutic window is narrow. The partial hepatectomy model [13, 14], which is often combined with liver ischemia, is difficult to reproduce because there are currently no uniform criteria for hepatectomy volume.

Complete or partial ischemic models can be developed by means of permanent [15] or temporary [16–18] hepatic artery ligation with portal–vena cava shunting. In these models, blockage of blood flow into the liver leads to hepatic ischemia, in turn leading to hepatocyte necrosis. Subsequent liver failure is associated with the pathological release of inflammatory toxins, simulating the processes that occur during human liver failure. Therefore, ischemia model is the most commonly utilized animal model of liver failure [19].

The ischemic models utilized in previous studies have all relied on portocaval shunting using portocaval side-to-side [16], or end-to-side anastomosis [20, 21]. However, the procedure is time-consuming and difficult to perform; therefore, it cannot be widely adopted. Currently, there are no reports of hepatic failure in cases of portal vein preservation. In addition, the criteria for animal models of acute liver failure have been established before [22, 23]. The criteria are as follows: (a) potential reversibility, (b) reproducibility, (c) death due to liver failure, (d) use of large animals, (e) a suitable therapeutic window, (f) ethically appropriate methods, (g) minimal hazards to research personnel, (h) physiological metabolism similar to that of humans, and (i) changes in consciousness. Therefore, in the present study, we sought to determine whether the portal vein can be preserved to create a simplified and reproducible model of liver failure in large animals and compliance with the criteria above.

We present the following article in accordance with the ARRIVE 1.0 reporting checklist.

## Materials and Methods

### Animals

Eighteen Bama miniature pigs weighing between 35 and 45 kg (age, 12–24 months) were used for the experiments in the present study. They received humane care in accordance with the standard animal care guidelines established by the Laboratory Animal Management Association of China. Each pig was housed in an individual metal cage and was provided with a quiet and comfortable environment. They were fed three times a day with *ad libitum* access to drinking water. All procedures involving animals were reviewed and approved by the Institutional Animal Care and Use Committee of Beijing City (IACUC protocol number: SYXK (Beijing, China) 2018-0011).

The authors are accountable for all aspects of the work in ensuring that questions related to the accuracy or integrity of any part of the work are appropriately investigated and resolved. Experiments were performed under a project license (NO.: 201912001) granted by the institutional review board of Nongong (Beijing, China) Life Science and Technology Co., in compliance with EU Directive 2010/63/EU for the care and use of animals.

### Experimental groups

The study design is presented in Fig. 1. Eighteen pigs were randomly divided into three intervention groups according to different degrees of portal vein constriction after ligation of the common bile duct and hepatic artery based on the results of our preliminary experiments. The number of animals in each group was determined based on similar research reports [14]. The study groups and the degree of portal vein constriction were as follows: group A (n=6), non-constricted; group B (n=6), reduction

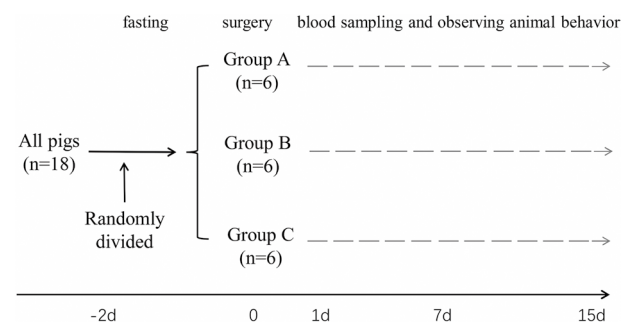


**Fig. 1.** Study design. All pigs were randomly divided into three intervention groups. The experimental timeline shown here presents the sequence of events to establish the acute liver failure (ALF) models.

of the portal vein perimeter by 1/3 based on a perimeter equal to  $2\pi r$  ( $r$ , radius) and a circular area equal to  $\pi r^2$ , resulting in the narrowing of the cross-sectional area by 4/9; and group C ( $n=6$ ), reduction of the portal vein perimeter by 1/2, resulting in the narrowing of the cross-sectional area by 3/4.

### Surgical procedures

**General care and anesthesia:** Prior to surgery, the pigs were starved for 12 h, although they were allowed *ad libitum* access to water until 4 h before the operation. Anesthesia was induced via an intramuscular injection of midazolam (0.1 mg/kg) and sodium pentobarbital (20 mg/kg). The pigs were placed in the supine position after disappearance of the eyelid reflex, after which they were intubated and connected to an anesthetic ventilator to ensure continuous inhalation of isoflurane (1–2%) and O<sub>2</sub> (2 L/min). The tidal volume of the anesthetic machine was set to 8–12 ml/kg, and the respiratory rate was adjusted based on the end-expiratory partial pressure of CO<sub>2</sub>, which was maintained at 35–45 mmHg. Following intubation, the right internal jugular vein was cannulated with a double-lumen catheter (Supplementary Fig. 1) to connect a venous pressure meter, which allowed monitoring of the central venous pressure (CVP). The catheter was also used for blood sampling and perfusion treatment. The right common carotid artery was also cannulated to monitor arterial pressure. Continuous intravenous infusions of propofol (6–8 mg/kg/h) and fentanyl (0.015 mg/kg/h) were administered for analgesia, while atracurium (no more than 0.7 mg/kg/h) was administered to ensure muscle relaxation. Echocardiography was performed, and the following vital signs were closely monitored and recorded: rectal temperature (T), heart rate (HR), mean arterial pressure (MAP), CVP, and peripheral oxygen saturation (SpO<sub>2</sub>).

**Surgery:** A midline laparotomy was performed to enable entry into the abdominal cavity, following which the intestines were pushed to the lower left abdomen. A deep automatic retractor was used to fully expose the right upper quadrant of the abdominal cavity. The size, texture, and color of the liver were noted, and a 0.5 cm × 0.5 cm × 0.5 cm tissue sample was removed for histological analysis at baseline. The liver was skeletonized, and all structures in the hepatogastric and hepatoduodenal ligaments were dissected (Fig. 2A). The common bile duct, hepatic artery, and portal vein were then isolated, following which the common bile duct and hepatic artery were ligated and disconnected. The portal vein was preserved and left unprocessed in group A. In groups B and C, the perimeter of the portal vein above the confluence of the splenic vein was measured using

silk thread (Figs. 2B and C), following which the portal vein was constricted using No. 7 silk thread, which two knots was made on the silk thread as markers and the distance between the two marked knots is the shortened perimeter length (Fig. 2D), to reduce its perimeter by 1/3 and 1/2, respectively (Fig. 2F). Such constriction decreased the hepatic blood supply, resulting in hepatic ischemia. The color and movement of the intestines were monitored. When there was no obvious congestion and intestinal motility was sufficient, the abdomen was washed with 1 L of warm physiological saline. A continuous suture was then used to close the skin and subcutaneous tissue.

**Postoperative monitoring:** Vital signs were closely monitored after surgery. Crystal and colloid fluid volumes were adjusted to maintain hemodynamic stability. Once a pig could breathe on its own for 30 min, the tracheal tube was removed if its vital signs were stable. Animals continued to receive intensive care and analgesic treatment with intravenous infusions of flurbiprofen axetil (50 mg/day) after surgery. They were allowed water *ad libitum*. The liquid input and supplementary energy were calculated according to the body weight, the total liquid input was 50 ml/kg/day and the energy was 30 kcal/kg/day. The ratio of sugar to fat was 1:1 to supplement energy. Catheters were flushed twice daily with about 10 ml heparinized saline (10 U/ml).

### Survival

In our preliminary experiment, all pigs with unprocessed portal veins survived for >1 month. Postoperative day 15 was selected as the endpoint for group A. Pigs in groups B and C were humanely euthanized by injection of pentobarbital and 10% potassium chloride, when they lapsed into a coma accompanied with tachypnea. Survival time was recorded as the time interval from completion of surgery to the time when the animals were sacrificed.

### Clinical observation and encephalopathy scores

The behavioral status of each pig was recorded each day after surgery. The animals were scored using the Encephalopathy Score Table created by Inge Fourneau [16], which is used to assess general behavior, gait, drinking, and eye-opening responses. The detailed scoring items and corresponding scores are shown in Table 1. Data were collected daily for all pigs until they were euthanized.

### Blood sampling

Preoperative venous blood was collected to determine baseline values, while fasting venous blood was col-



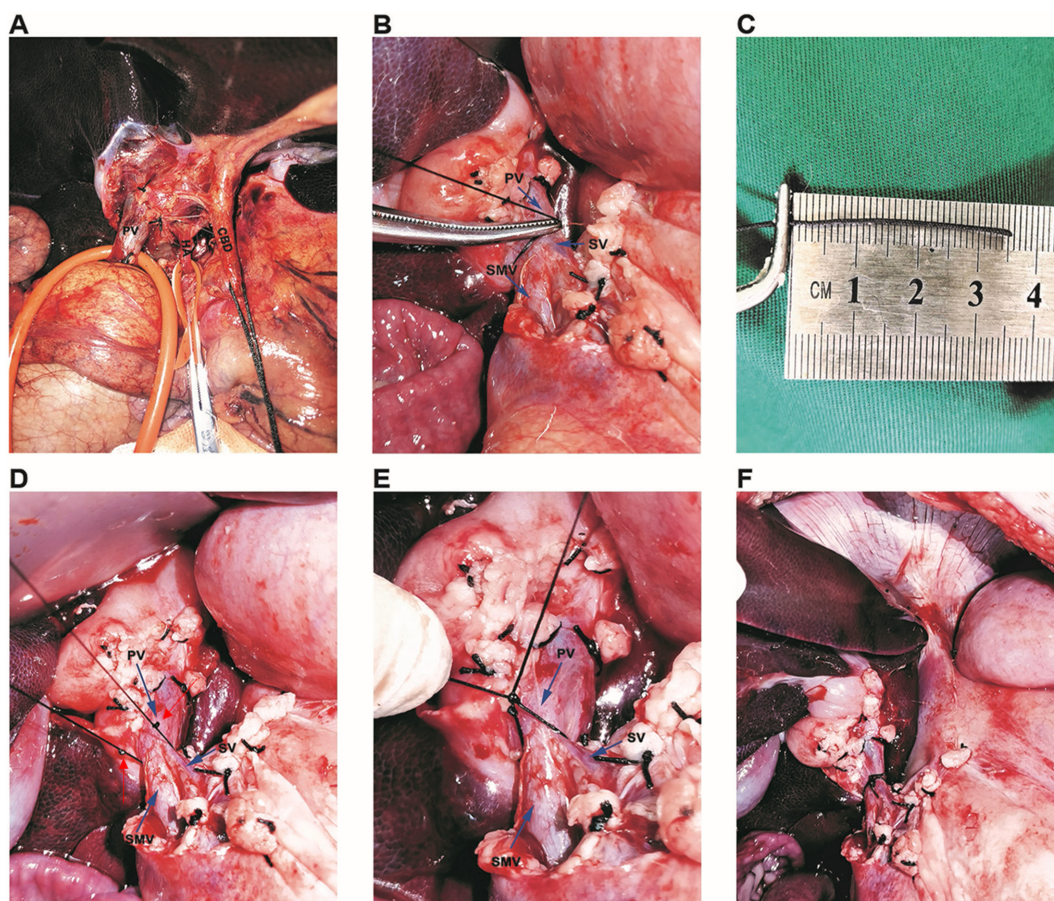


**Fig. 2.** Simple surgical procedures for portal vein preservation combined with common bile duct and hepatic artery ligation and transection. (A) Isolation and skeletonization of the portal vein, hepatic artery, and common bile duct. (B–C) Measurement of the perimeter of the portal vein after ligation and transection of the common bile duct and hepatic artery. (D) Two knots (red arrow) were made on the silk thread as markers, the distance between the two marked knots is the shortened perimeter length. (E) Constriction of the portal vein. (F) Completion of surgery. CBD, common bile duct; PV, portal vein; HA, hepatic artery; SV, splenic vein.

lected each morning until the animals died. Biochemical analyses for the levels of the following macromolecules were performed immediately after obtaining blood samples: alanine aminotransferase (ALT), aspartate aminotransferase (AST), lactate dehydrogenase (LDH), alkaline phosphatase (ALP), total bilirubin (TBiL), direct bilirubin (DBiL), ammonia (Amm), albumin (ALB), creatinine (Cr), blood urea nitrogen (BUN), glucose (Glu), and blood lactate (Lac).

### Histological examination

Autopsies were performed immediately after the pigs died. The Patency of the portal vein was carefully inspected. Tissues were dissected, and formalin was used for fixation. Routine sampling, dehydration, embedding, and sectioning were performed. After sectioning, hematoxylin–eosin (HE) staining, Masson trichrome staining, terminal deoxynucleotidyl transferase-mediated dUTP nick-end labeling (TUNEL) staining, and Ki-67 immunohistochemical staining were performed to assess the

**Table 1.** Encephalopathy scoring system

Variable	Points
General behavior	
Quiet and awake	5
Somnolent	4
Restless	3
Soporose	2
Comatose	1
Gait	
Normal	3
Cerebellar	2
No	1
Drinking	
Spontaneous	3
On presentation	2
No	1
Eye opening	
Spontaneous	4
On stimulus	
Acoustic	3
Painful	2
No	1

extent of pathological changes in the liver, hepatic fibrosis, hepatocyte apoptosis, and hepatocyte proliferation, respectively.

### Statistical analysis

Numerical data are reported as means  $\pm$  SD. One-way analyses of variance were used to compare the means among the three groups. A paired-sample t-test was used to compare the data with baseline measurements. The Kaplan–Meier method was used to analyze differences in survival. All data were analyzed using SPSS version 26.0 (SPSS, IBM, Chicago, IL, USA). The level of statistical significance was set to  $P < 0.05$ .

## Results

### Surgical outcomes

Surgery was successful in all animals. Surgical outcomes for all three groups are shown in Table 2. Vital signs were stable throughout the procedure in groups A and B. When the portal vein was constricted, the values of MAP, CVP, and HR changed significantly in group C when compared with baseline values ( $P < 0.01$  for all): MAP and CVP decreased, whereas HR tended to increase. Intraoperative changes in T, HR, MAP, CVP, and SpO<sub>2</sub> in each group are shown in Figs. 3A–E.

### Survival

All pigs in group A survived to postoperative day 15. In group B, the shortest duration of survival was 9 days, while the longest duration of survival was 14 days. The mean survival time was  $11.67 \pm 1.86$  days. Survival times were significantly shorter in group C than in the other two groups, as all animals in group C died within 3 days of surgery (mean survival:  $2.16 \pm 0.75$  days). Kaplan–Meier survival analysis revealed significant differences in survival time among the groups ( $P < 0.001$ ). The survival curve is shown in Fig. 4A.

### Clinical assessment and encephalopathy scores

Significant differences in clinical manifestations were observed among the three groups. After surgery, the pigs in group C rapidly developed fatigue, depression, and cerebellar gait, following which they lost the ability to stand, became drowsy, and fell into a coma. The pigs in group B gradually developed fatigue, depression, and cerebellar gait, and their ability to drink water gradually decreased. Thereafter, eye-opening responses gradually disappeared. The pigs in group A remained capable of moving and drinking water freely. Encephalopathy scores for the different groups are shown in Fig. 4B.

### Biochemical analyses

After surgery, the levels of liver enzymes (ALT, AST, LDH, and ALP) significantly increased in all animals. However, significantly greater increases were observed in group C than in groups A and B (all  $P < 0.05$ ). The peak ALT values in groups A, B, and C were  $746.67 \pm 157.69$ ,  $720.00 \pm 357.44$ , and  $1,675.50 \pm 762.34$  U/L, respectively, whereas the peak AST values were  $2,890.00 \pm 790.65$ ,  $3,164.17 \pm 1,839.10$ , and  $7,938.00 \pm 3,747.73$  U/L, respectively. In groups A and B, liver enzyme levels decreased after reaching their peak at 2–4 days post-operatively; the peak appeared earlier in group B than in group A. TBIl and DBiL increased progressively in all groups when compared with baseline values ( $P < 0.05$  for all); they all reached their peak at the end point. These data, together with the changes in liver enzymes, suggest that bile enzyme separation occurred in groups A and B. Amm levels increased significantly relative to the baseline values in all groups after surgery ( $P < 0.05$  for all groups); however, the values were significantly lower in Group A than in groups B and C. ALB levels tended to decrease after surgery in all three groups ( $P < 0.05$  for all), with groups C and A having the fastest and slowest decreases, respectively. The levels of Cr and BUN, which are indicators of renal function, did not significantly change in groups A and B, although they increased after

**Table 2.** Basic characteristics of surgery

Items	Results			
	Group A	Group B	Group C	<i>P</i> value
Operative time (min)	$38.83 \pm 2.23$	$45.17 \pm 3.54$	$46.00 \pm 1.79$	$<0.001$
Operative time in LH (min) <sup>a</sup>	$12.00 \pm 1.10$	$14.33 \pm 1.03$	$14.00 \pm 1.41$	0.008
Perimeter of portal vein before occlusion (cm)	$3.69 \pm 0.13$	$3.68 \pm 0.06$	$3.72 \pm 0.09$	0.576
Perimeter of portal vein after occlusion (cm)	$3.69 \pm 0.13$	$2.50 \pm 0.44$	$1.87 \pm 0.50$	$<0.001$
ABL during the operation (mL)	$2.0 \pm 2.45$	$3.67 \pm 2.94$	$3.50 \pm 2.26$	0.984
ABT during the operation (mL)	0	0	0	1

Data are presented as means  $\pm$  SD,  $n=6$ ; LH, liver hilum; ABL, amount of blood loss; ABT, amount of blood transfusion.  
<sup>a</sup>Operative time in LH: including ligament separation, ligation of the hepatic artery and common bile duct, and portal vein constriction.

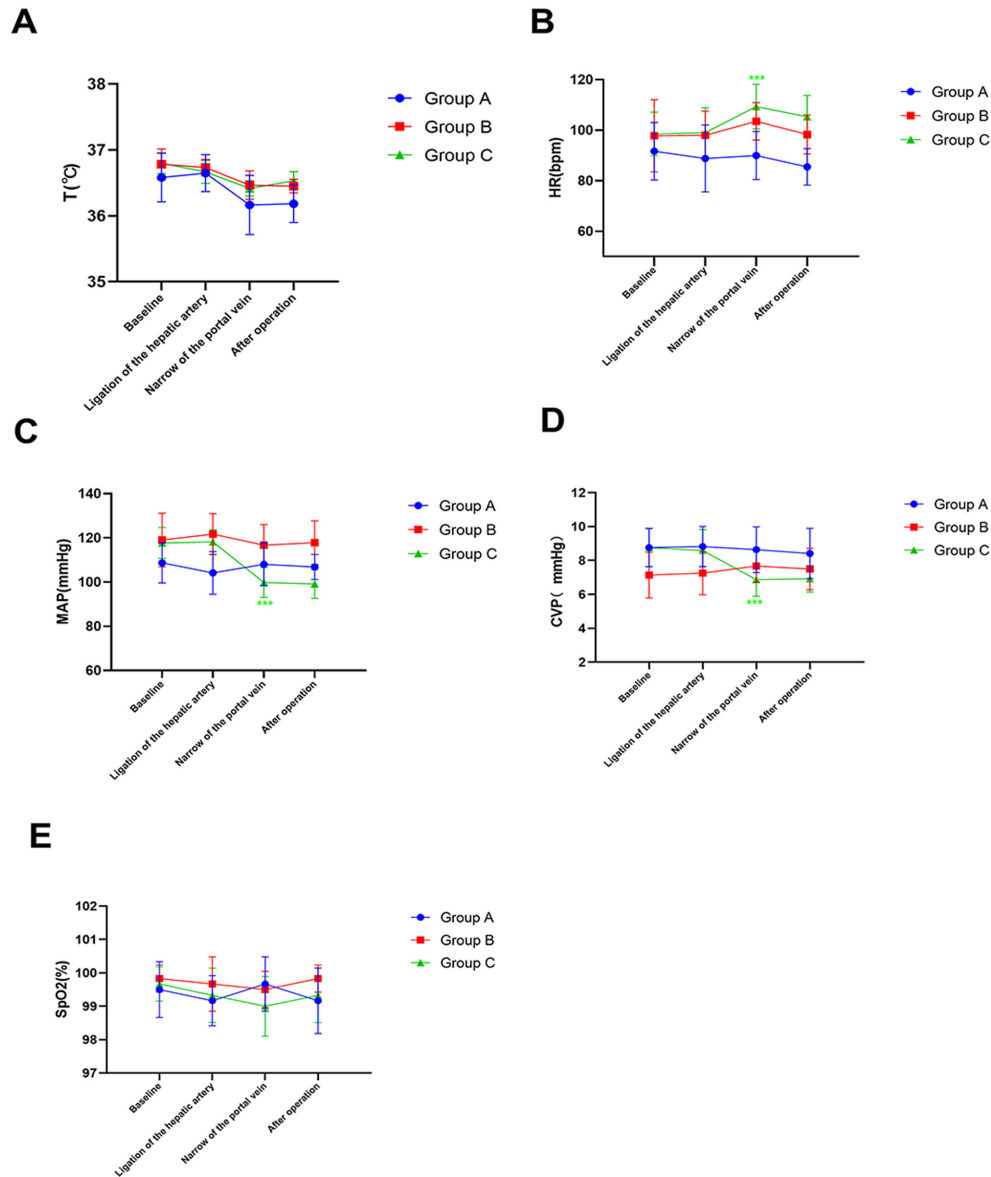


**Fig. 3.** Intraoperative changes of vitals. Changes in T (A), HR (B), MAP (C), CVP (D), and SpO<sub>2</sub> (E) during surgery in each group. Data are presented as means  $\pm$  SD; n=6; \*\*\* $P$ <0.001 versus baseline. T, rectal temperature; HR, heart rate; MAP, mean arterial pressure; CVP, central venous pressure; SpO<sub>2</sub>, peripheral oxygen saturation.

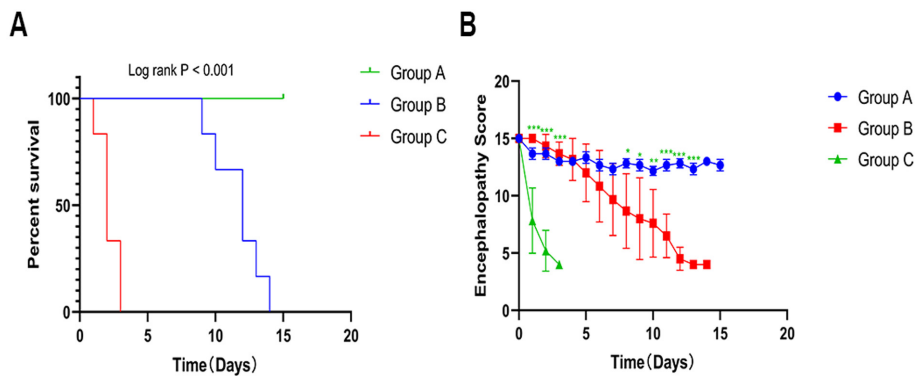


**Fig. 4.** Survival and encephalopathy score. (A) Survival times of pigs in the different study groups. Group A vs. group B,  $P$ <0.001; group A vs. group C,  $P$ <0.001; group B vs. group C,  $P$ <0.001. (B) Evolution of the encephalopathy score in the three groups. Data are presented as means  $\pm$  SD; n=6. \* $P$ <0.05, \*\* $P$ <0.005, \*\*\* $P$ <0.001, one-way analysis of variance.



surgery in group C ( $P<0.05$ ). Lac levels fluctuated steadily at low values in group A throughout the experimental observation process. In group B, Lac levels remained at low values in the early stage but rose rapidly within 3 days before the animals died. In contrast, group C exhibited progressive increases in Lac levels after surgery. Changes in biochemical and lactic acid values are shown in Figs. 5A–L.

### Morphological characteristics

A moderate amount of effusion was observed upon opening the abdominal cavity after the animals' death.

There was no congestion in the gastrointestinal. In group A, livers were yellowish brown with marked hepatomegaly and the hardened liver tissues exhibited obvious cholestasis. We also observed severe adhesions to the surrounding tissues and small nodules/granules on the surface of the liver in group A (Fig. 6A). In group B, livers were dark brown, and obvious cholestasis was observed in some areas. The tissue was brittle, hard, and fractured easily, with some adhesions to the surrounding tissues (Fig. 6B). In group C, livers were dark purple and yellowish brown, while their surfaces were softer and smoother. Fewer adhesions to the surrounding tissue

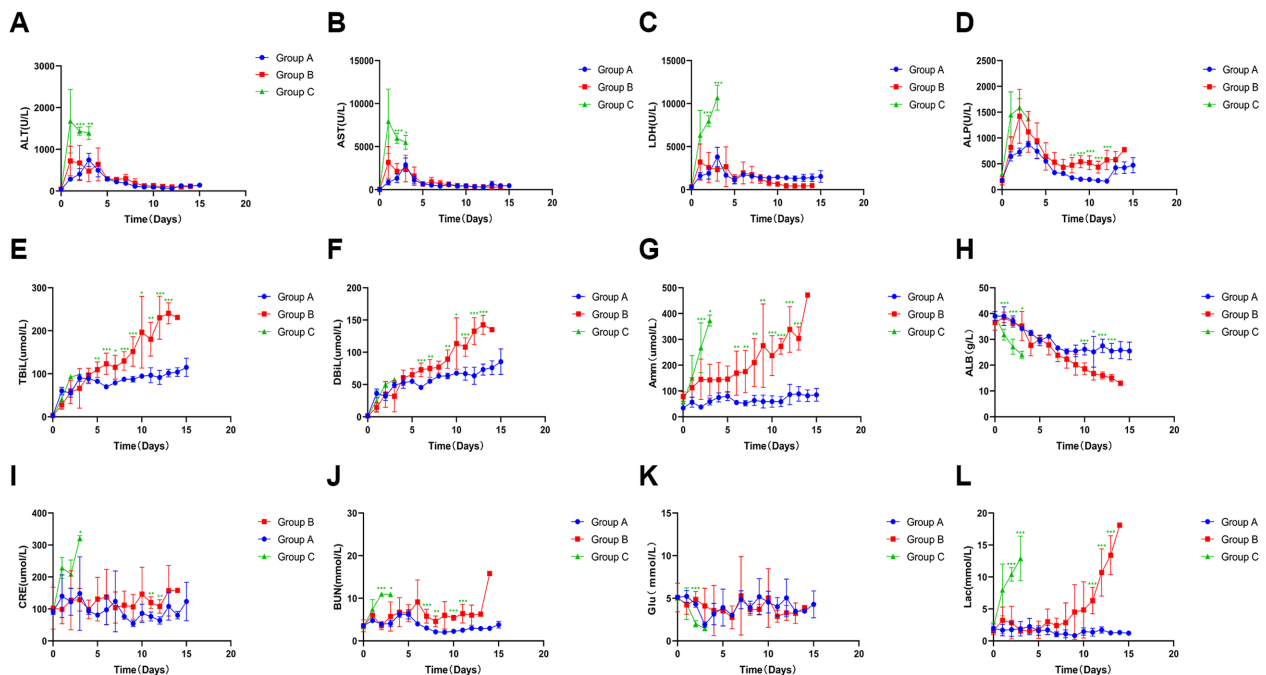


**Fig. 5.** Biochemical analysis. Changes in the levels of ALT (A), AST (B), LDH (C), ALP (D), TBiL (E), DBiL (F), Amm (G), ALB (H), Cr (I), BUN (J), Glu (K), and Lac (L) prior to the operation (baseline) and each day after the operation. Data are presented as means  $\pm$  SD,  $n=6$ . \* $P<0.05$ , \*\* $P<0.005$ , \*\*\* $P<0.001$ , one-way analysis of variance. ALT, alanine aminotransferase; AST, aspartate aminotransferase; LDH, lactate dehydrogenase; ALP, alkaline phosphatase; TBiL, total bilirubin; DBiL, direct bilirubin; Amm, ammonia; ALB, albumin; Cr, creatinine; BUN, blood urea nitrogen; Glu, glucose; Lac, blood lactate.

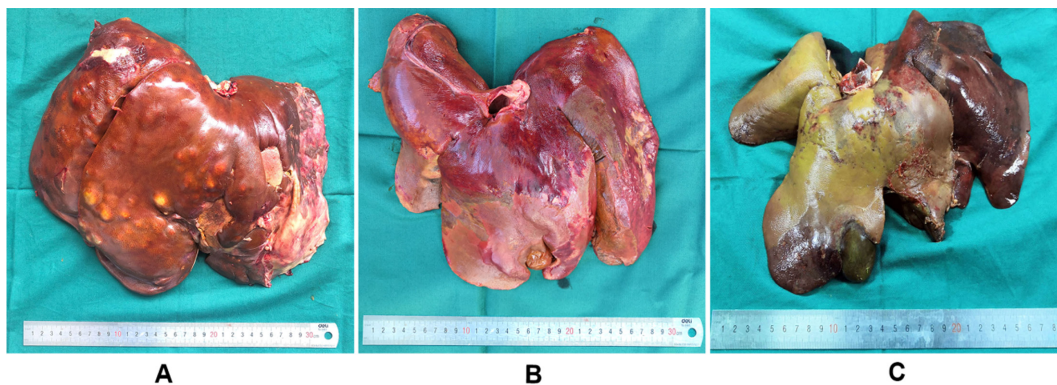


**Fig. 6.** Morphological characteristics of the liver. A, Group A, livers were yellowish brown with marked hepatomegaly; B, Group B, livers were dark brown, and obvious cholestasis was observed in some areas; C, livers were dark purple and yellowish brown.

were observed in group C (Fig. 6C). At autopsy, no thrombosis of the portal vein was noted in all animals.

### Histological characteristics

Animals in each group exhibited varying degrees of liver damage relative to the baseline condition. In group A, the lobular structure had collapsed, while moderate hepatocyte necrosis and infiltration of the surrounding inflammatory cells were observed. Moreover, we noted substantial proliferation of fibrous tissues and Ki-67 immunostaining revealed significant increases in hepatocyte proliferation. In group B, the lobular structure had also collapsed, while massive fused necrosis of hepatocytes was observed. Substantial infiltration of surrounding inflammatory cells was accompanied by the disappearance of necrotic cells, balloon-like changes, and vacuolar degeneration. Masson staining revealed severe fibrosis, whereas Ki-67 immunostaining revealed scattered hepatocyte proliferation. In addition, cholestasis was observed both in group A and B. In group C, the lobular structure was basically intact, and small amounts

of necrosis and balloon-like changes were observed. There was no evidence of fibrous tissue proliferation, and Ki-67 immunostaining revealed slight hepatocyte proliferation at the lobular margin. TUNEL staining was observed in all groups, while levels of TUNEL staining in all experimental groups were similar to those observed at baseline. The histological characteristics of the liver for each group are shown in Fig. 7.

### Discussion

We succeeded in developing a novel, simplified, and reproducible porcine model of ischemic liver failure with portal vein preservation in compliance with the criteria for animal models of acute liver failure.

In this study, a portal vein-preserving model of partial ischemic liver failure was established for the first time. By ligating the hepatic artery and contracting the portal vein, the blood flow to the liver decreases sharply, which leads to hepatocellular necrosis caused by ischemia and hypoxia and eventually to the rapid loss of normal liver

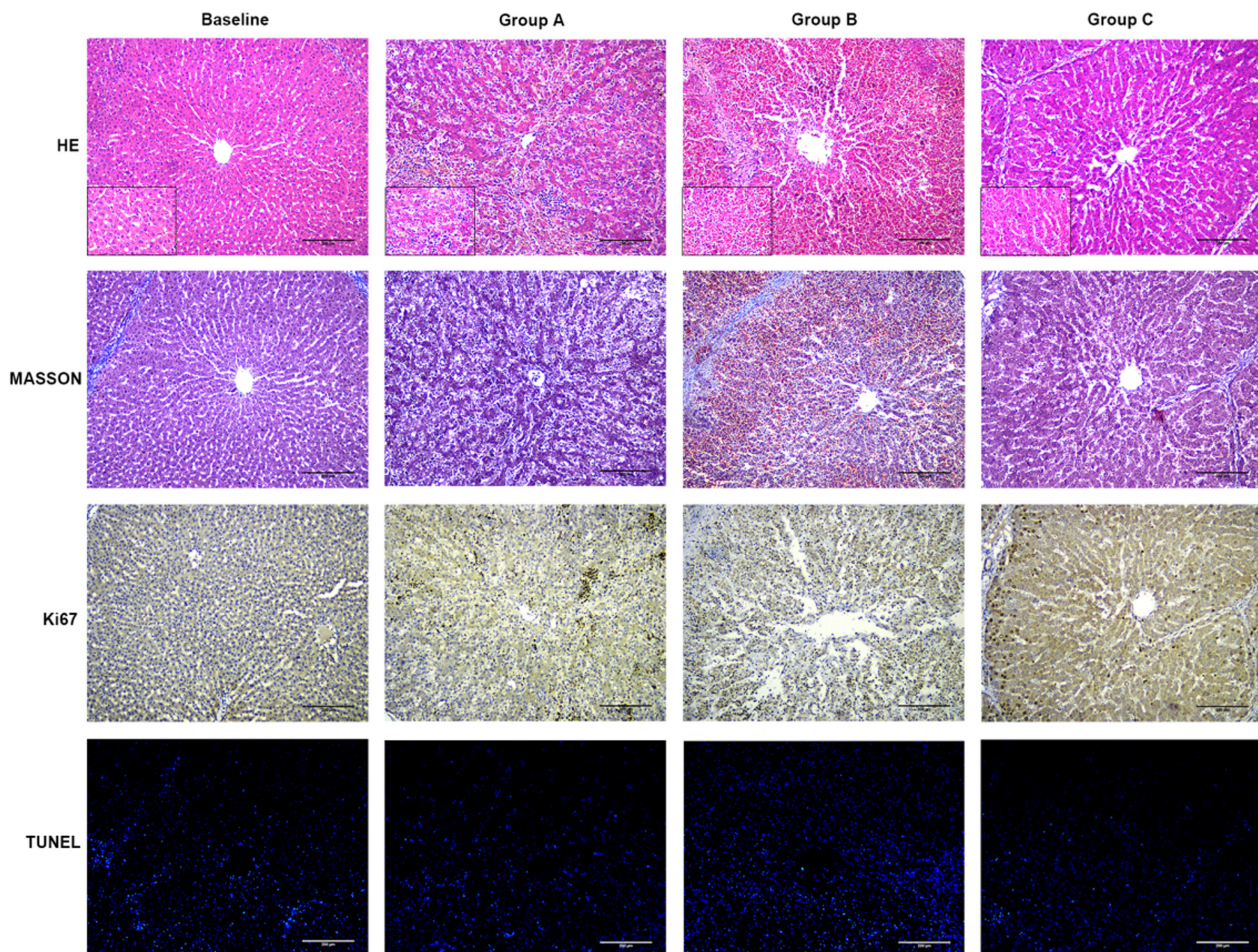


**Fig. 7.** Liver histology and immunohistochemistry from baseline and of the different groups. HE, hematoxylin-eosin; TUNEL, terminal deoxynucleotidyl transferase dUTP nick-end labeling ( $\times 100$  magnification,  $200\text{-}\mu\text{m}$  scale bars).



function. Previous studies have shown that the collateral circulation of the bile duct wall can provide blood flow to the liver [17, 24], which is very important. Without ligation, the survival time of liver failure model animals will be significantly prolonged [16]. In order to avoid the effect of collateral circulation on hepatic ischemia, the model animals of hepatic failure were subjected to ligation and disconnection of the common bile duct. More importantly, after ligation of the common bile duct, bilirubin and bile acid accumulate due to the loss of the liver's excretory function, leading to inflammation and liver failure [21].

Compared with other partial ischemia models, this model does not require portocaval shunting, is easy to operate, and is time-saving. The portal vein occlusion time was 11 to 15 min, as previously reported [15]. Although we modified the portocaval shunting method by using a polyvinyl chloride tube to bridge the portal vein and vena cava, the portal vein blood flow was also blocked for  $5 \pm 2$  min [9]. To simplify the operation, the portal vein preserving liver failure model developed in this study does not require occlusion of this vein or portal shunting.

The key to establishing the model is to determine the appropriate degree of portal vein constriction. In a preliminary experiment involving more than 10 pigs, we explored different degrees of portal vein contraction, including non-constriction, reduced 1/5, 1/4, 1/3, or 1/2, and completely blocked portal vein perimeters, respectively, and compared their biochemical and survival time. Preliminary studies have shown that excessive preservation of cross-sectional area can significantly slow down the development of liver failure and prolong the survival time. The survival time of pigs without portal vein stenosis was more than 1 month, and the main cause of death was severe hyperbilirubinemia. However, gastrointestinal congestion and severe hemodynamic fluctuations occur when the portal vein cross-sectional area is reduced (>75%). When the portal vein was completely blocked, the animals died within 5 h. According to preliminary data, three different degrees of portal vein stenosis were investigated in this study.

Biochemical changes and survival time are important in evaluating the success of animal models of liver failure. In this study, different degrees of portal vein constriction in the animal model showed a statistically significant difference in survival time and biochemical indicators. In group C, ALT, AST, Amm, Lac, CRE, and BUN increased significantly, while ALB decreased significantly, suggesting liver function and multiple organ failure. The change in trends of some indicators between group A and group B were similar; ALT, AST, LDH, ALP

increased first but then decreased, ALB gradually decreased, and TBIL and DBIL gradually increased, which suggested that liver failure developed in both groups. However, the changes of ALB, TBIL, and DBIL in group B were significantly larger than those in group A, and more importantly, Amm and Lac increased significantly postoperatively in group B. However, these two indicators in group A remained at a low level during the observation period. We considered all the changes to be related to different degrees of hepatic ischemia induced by different coarctations of the portal vein in the three groups. Although the biochemical indexes of group C seemed to change significantly, its survival time was excessively short, resulting in an inappropriate therapeutic window. Both groups A and B had suitable therapeutic window time, and some biochemical indexes were similar. However, since blood ammonia and lactate are important in the treatment of liver failure, we believe that reducing the portal vein perimeter by 1/3 may be the most appropriate strategy.

Neurological changes are another important indicator when evaluating animal models of liver failure [25]. These changes can be assessed by utilizing the Encephalopathy Score Table developed by Fourneau *et al.* [16]. Encephalopathy scores were negatively correlated with Amm levels, consistent with previously reported hypotheses [26]. The two indices of group B and group C had significant changes, indicating that consciousness had changed. However, encephalopathy scores and Amm levels remained stable in group A. These results and pathological findings suggest that the preservation of portal vein can make the liver retain enough hepatocytes to maintain metabolic capacity.

The morphological and pathological changes of the liver were different among the groups. In group C, although the liver morphology changed, the pathological changes were not obvious. The lobule structure was basically intact with only a few necroses. This may be related to the short survival time of group C. The large contraction area of the portal vein leads to hemodynamic changes and, eventually, to the death of model pigs shortly. However, the liver cells have a strong ability to tolerate ischemia and hypoxia [17], and the typical necrosis of liver cells has not yet appeared during this time. In addition, the observation time was insufficient to observe for cell proliferation and fibrous hyperplasia in the liver. Based on these evidences, group C is not suitable to be regarded as a liver failure model, and may be more suitable to be regarded as a hemodynamic failure model. Under long-term ischemic hypoxic conditions in groups A and B, the livers in both groups exhibited obvious proliferation and fibrosis, and hepatocytes ex-

hibited obvious necrosis and destruction of lobular architecture. Although the two groups performed similarly, the degree of hepatocellular necrosis and lobular structure damage in group B were significantly higher than those in group A.

In the current study, the perimeter was chosen as the experimental variable, considering its reproducibility and convenience of measurement. In our supplementary experiments, we detected the changes of portal vein blood flow caused by reducing portal vein perimeter in different degrees using 6 pigs. The results showed that when the portal vein perimeter reduced by 1/3, the portal vein blood flow decreased from an average of  $942.94 \pm 201.16$  ml/min to  $534.02 \pm 97.39$  ml/min, while when the portal vein perimeter reduced by 1/2, the portal vein blood flow decreased from an average of  $851.34 \pm 5.00$  ml/min to  $387.87 \pm 15.66$  ml/min. Demonstrated that portal vein blood flow closely related to its' perimeter and portal vein perimeter can be used as the marker of this model. However, more animal experiments are needed to determine the relationship between portal vein perimeters and blood flow. Daily heparin injections may prevent jugular catheter and portal vein thrombosis, leading to impaired coagulation function testing. Therefore, changes in coagulation in liver failure could not be demonstrated.

### Conclusion

The novel partial ischemic model of portal vein constriction developed in the present study effectively mimics the clinical characteristics of acute liver failure in humans. Furthermore, we successfully validated the various manifestations of different degrees of portal vein constriction. This model is highly reproducible and easy to generate. We believe that this model may help provide a platform for further research related to the development of ALSS.

### Acknowledgments

This work was supported by the National Key R&D Program of China (2018YFC1106400; 2018YFA0108200), Science and Technology Planning Project of Guangdong Province (2015B020229002), the National Natural Science Foundation of China (31972926), the Natural Science Foundation of Guangdong Province (2014A030312013, 2018A030313128), Guangdong Key Research and Development Plan (2019B020234003), and Science and Technology Program of Guangzhou (201803010086).

### References

- Choudhary NS, Saraf N, Saigal S, Sooin AS. Factors Associated With Survival of Patients With Severe Acute-On-Chronic Liver Failure Before and After Liver Transplantation: Unanswered Questions. *Gastroenterology*. 2019; 157: 1162–1163. [[Medline](#)] [[CrossRef](#)]
- Schlegel A, Muller X, Kalisvaart M, Muellhaupt B, Perera MTPR, Isaac JR, et al. Outcomes of DCD liver transplantation using organs treated by hypothermic oxygenated perfusion before implantation. *J Hepatol*. 2019; 70: 50–57. [[Medline](#)] [[CrossRef](#)]
- Zhang Z, Zhao YC, Cheng Y, Jian GD, Pan MX, Gao Y. Hybrid bioartificial liver support in cynomolgus monkeys with D-galactosamine-induced acute liver failure. *World J Gastroenterol*. 2014; 20: 17399–17406. [[Medline](#)] [[CrossRef](#)]
- Chen S, Wang J, Ren H, Liu Y, Xiang C, Li C, et al. Hepatic spheroids derived from human induced pluripotent stem cells in bio-artificial liver rescue porcine acute liver failure. *Cell Res*. 2020; 30: 95–97. [[Medline](#)] [[CrossRef](#)]
- Gravante G, Ong SL, McGregor A, Sorge R, Metcalfe MS, Lloyd DM, et al. Histological changes during extracorporeal perfusions of the porcine liver: implications for temporary support during acute liver failures. *J Artif Organs*. 2013; 16: 218–228. [[Medline](#)] [[CrossRef](#)]
- Kumar A, Tripathi A, Jain S. Extracorporeal bioartificial liver for treating acute liver diseases. *J Extra Corpor Technol*. 2011; 43: 195–206. [[Medline](#)]
- Akagunduz B, Ozer M, Ozcicek F, Kara AV, Lacin S, Özkaraca M, et al. Protective effects of taxifolin on pazopanib-induced liver toxicity: an experimental rat model. *Exp Anim*. 2021; 70: 169–176. [[Medline](#)] [[CrossRef](#)]
- Feng L, Cai L, He GL, Weng J, Li Y, Pan MX, et al. Novel D-galactosamine-induced cynomolgus monkey model of acute liver failure. *World J Gastroenterol*. 2017; 23: 7572–7583. [[Medline](#)] [[CrossRef](#)]
- Cai L, Weng J, Feng L, He G, Qin J, Zhang Z, et al. Establishment of a Novel Simplified Surgical Model of Acute Liver Failure in the Cynomolgus Monkey. *BioMed Res Int*. 2016; 2016: 3518989. [[Medline](#)] [[CrossRef](#)]
- Miller DJ, Hickman R, Fratter R, Terblanche J, Saunders SJ. An animal model of fulminant hepatic failure: a feasibility study. *Gastroenterology*. 1976; 71: 109–113. [[Medline](#)] [[CrossRef](#)]
- Siellaf TD, Hu MY, Rollins MD, Bloomer JR, Amiot B, Hu WS, et al. An anesthetized model of lethal canine galactosamine fulminant hepatic failure. *Hepatology*. 1995; 21: 796–804. [[Medline](#)]
- Sosef MN, Abrahamse LS, van de Kerkhove MP, Hartman R, Chamuleau RA, van Gulik TM. Assessment of the AMC-bioartificial liver in the anhepatic pig. *Transplantation*. 2002; 73: 204–209. [[Medline](#)] [[CrossRef](#)]
- Yu Y, Tamai M, Tagawa YI. Nitric oxide is critical for avoiding hepatic lipid overloading via IL-6 induction during liver regeneration after partial hepatectomy in mice. *Exp Anim*. 2017; 66: 293–302. [[Medline](#)] [[CrossRef](#)]
- Chen HS, Joo DJ, Shaheen M, Li Y, Wang Y, Yang J, et al. Randomized Trial of Spheroid Reservoir Bioartificial Liver in Porcine Model of Posthepatectomy Liver Failure. *Hepatology*. 2019; 69: 329–342. [[Medline](#)] [[CrossRef](#)]
- Ytrebø LM, Nedredal GI, Langbakk B, Revhaug A. An experimental large animal model for the assessment of bioartificial liver support systems in fulminant hepatic failure. *Scand J Gastroenterol*. 2002; 37: 1077–1088. [[Medline](#)] [[CrossRef](#)]
- Fourneau I, Pirenne J, Roskams T, Yap SH. An improved model of acute liver failure based on transient ischemia of the liver. *Arch Surg*. 2000; 135: 1183–1189. [[Medline](#)] [[CrossRef](#)]
- de Groot GH, Reuvers CB, Schalm SW, Boks AL, Terpstra

- OT, Jeekel H, et al. A reproducible model of acute hepatic failure by transient ischemia in the pig. *J Surg Res.* 1987; 42: 92–100. [[Medline](#)] [[CrossRef](#)]
18. Fischer M, Stötter L, Schmahl W, Gartmaier P, Erhardt W. Acute liver failure due to temporary hepatic ischemia in the pig. *Acta Hepatogastroenterol (Stuttg).* 1976; 23: 241–249. [[Medline](#)]
  19. Nieuwoudt M, Kunnike R, Smuts M, Becker J, Stegmann GF, Van der Walt C, et al. Standardization criteria for an ischemic surgical model of acute hepatic failure in pigs. *Biomaterials.* 2006; 27: 3836–3845. [[Medline](#)] [[CrossRef](#)]
  20. Rozga J, Williams F, Ro MS, Neuzil DF, Giorgio TD, Backfisch G, et al. Development of a bioartificial liver: properties and function of a hollow-fiber module inoculated with liver cells. *Hepatology.* 1993; 17: 258–265. [[Medline](#)] [[CrossRef](#)]
  21. Awad SS, Hemmila MR, Soldes OS, Sawada S, Rich PB, Mahler S, et al. A novel stable reproducible model of hepatic failure in canines. *J Surg Res.* 2000; 94: 167–171. [[Medline](#)] [[CrossRef](#)]
  22. Terblanche J, Hickman R. Animal models of fulminant hepatic failure. *Dig Dis Sci.* 1991; 36: 770–774. [[Medline](#)] [[CrossRef](#)]
  23. van de Kerkhove MP, Hoekstra R, van Gulik TM, Chamuleau RA. Large animal models of fulminant hepatic failure in artificial and bioartificial liver support research. *Biomaterials.* 2004; 25: 1613–1625. [[Medline](#)] [[CrossRef](#)]
  24. Benoist S, Sarkis R, Baudrimont M, Delelo R, Robert A, Vau-bourdolle M, et al. A reversible model of acute hepatic failure by temporary hepatic ischemia in the pig. *J Surg Res.* 2000; 88: 63–69. [[Medline](#)] [[CrossRef](#)]
  25. Franzoni LC, de Carvalho FC, Garzon RG, Yamashiro FS, Augusti L, Santos LA, et al. Embolization of splenorenal shunt associated to portal vein thrombosis and hepatic encephalopathy. *World J Gastroenterol.* 2014; 20: 15910–15915. [[Medline](#)] [[CrossRef](#)]
  26. Zieve L. The mechanism of hepatic coma. *Hepatology.* 1981; 1: 360–365. [[Medline](#)] [[CrossRef](#)]